Pharmaceutical Research, Vol. 25, No. 1, January 2008 (© 2007)
DOI: 10.1007/s11095-007-9355-8

Research Paper

Incorporation of Antitubercular Drug Isoniazid in Pharmaceutically Accepted Microemulsion: Effect on Microstructure and Physical Parameters

S. K. Mehta,[1,2] Gurpreet Kaur,[1] and K. K. Bhasin[1]

Received April 14, 2007; accepted May 18, 2007; published online June 19, 2007

Purpose. The purpose of present study is to formulate microemulsion composed of oleic acid, phosphate buffer, Tween 80, ethanol and to investigate its potential as drug delivery system for an antitubercular drug isoniazid.

Materials and Methods. The pseudo-ternary phase diagram (Gibbs Triangle) was delineated at constant surfactant/co-surfactant ratio (Km 0.55). Changes in the microstructure were established using conductivity (σ), viscosity (η), surface tension (γ) and density measurements. Dissolution studies and particle size analysis were carried out to understand the release of isoniazid from the microemulsion formulation. Further, partitioning studies and spectroscopic analysis (FT-IR and ^{1}H NMR) was performed to evaluate the location of drug in the colloidal formulation.

Results. Physico-chemical analysis of microemulsion system showed the occurrence of structural changes from water-in-oil to oil-in-water microemulsion. It has been observed that the microemulsion remained stable after the incorporation of isoniazid (in terms of optical texture, pH and phase separation). The changes in the microstructure of the microemulsion after incorporation of drug was analyzed on the basis of partition studies of isoniazid in microemulsion components and various parameters viz pH, σ, η,γ. In addition, the particle size analysis indicates that the microemulsion changes into o/w emulsion at infinite dilution. The spectroscopic studies revealed that most of the drug molecules are present in the continuum region of an o/w microemulsion. Dissolution studies infer that a controlled release of drug is expected from o/w emulsion droplet. In the present system the release of isoniazid from microemulsion was found to be non-Fickian.

Conclusion. The present Tween based microemulsion appears beneficial for the delivery of the isoniazid in terms of easy preparation, stability, low cost, sustained and controlled release of a highly water soluble drug.

KEY WORDS: controlled release; drug delivery potential; isoniazid; microemulsion; solubility; stability; structural changes.

INTRODUCTION

In order to enhance the efficacy of new and existing drugs, the design and development of new drug delivery systems is an ongoing process. Recently a great deal of focus has been laid on microemulsions (1,2) and self-microemulsifying drug delivery systems (SMEDDS) (3–6) for this purpose. SMEDDS is a preconcentrate of microemulsion containing drug, oil, and surfactant (and/or cosurfactant). It helps in enhancing solubility, dissolution rate and improves bioavailability of a drug (7).

Microemulsions are thermodynamically stable, isotropic clear dispersions of oil, water and surfactant (and/or co-surfactant) mixtures, which have high stability, low viscosity and transparency. Microemulsions are known for more than a half-century but it's only in the past decade that its ability as a drug delivery vehicle is being explored. Besides easy administration of microemulsion (when used as oral drug delivery systems), they help in increased absorption, improved clinical potency and decreased toxicity (8).

Some of the advantages associated with microemulsions as drug delivery systems are improvement of drug solubilization, protection against enzymatic hydrolysis, enhanced absorption due to surfactant induced permeability, increased penetration of hydrophilic, hydrophobic, amphiphilic substances (9–13), increase mobility (14,15) and favorable modification of therapeutic activity of drugs (16,17).

Microemulsion comprises different structures (water in oil (w/o), oil in water (o/w) and bicontinuous) and these structural changes help in preferential releasing of the drug (18). Because of presence of hydrophobic and hydrophilic component as part of structure, these systems may serve as vehicles for drugs of different solublities. To investigate the drug delivery potential of microemulsion vehicles, it is necessary to characterize the microstructure of pure and

Electronic supplementary material The online version of this article (doi:10.1007/s11095-007-9355-8) contains supplementary material, which is available to authorized users.

[1] Department of Chemistry and Center of Advanced Studies in Chemistry, Panjab University, Chandigarh, 160 014, India.

[2] To whom correspondence should be addressed. (e-mail: skmehta@pu.ac.in)

drug loaded microemulsion. The changes in the internal structure of a microemulsion can be monitored by analyzing conductivity, viscosity, density, surface tension and differential scanning calorimetry, etc (19). The incorporated drug may or may not influence the microstructure. O/w and w/o microemulsions may show different behavior for the release of both hydrophilic and lipophilic drugs. Release will be fast for a hydrophilic drug in case of an o/w microemulsion since it is in the continuum region. The diffusion is difficult when incorporated in w/o, since it gets trapped in water droplets. Reverse is true for hydrophobic drugs.

To construct a pharmaceutically accepted microemulsion it is important to know its physicochemical properties. For the selection of components of a biocompatible microemulsion system, the use of non-ionic surfactants has been widely accepted, since along with being compatible they retain its utility over a broad range of pH values and may affect the skin barrier function (18,20–23).

It is believed that the particle size of a drug is particularly important if the drug has low solubility. Moreover, the size of encapsulated particle is needed to be controlled to avoid blockage in the capillaries (24). Substances in the molecularly dispersed form are more efficiently absorbed into systemic circulation, since small particles (in the nanometer range) have high absorptive area, therefore they penetrate the cell membrane more efficiently (25). Since, microemulsion is projected to infinite dilution by body fluids (*in vivo* conditions), it becomes increasingly important to know the particle size (of pure and drug loaded microemulsion) and drug release at infinite dilution. It is found from the literature, the release of drugs in micelle and microemulsion system is diffusion-controlled release (26).

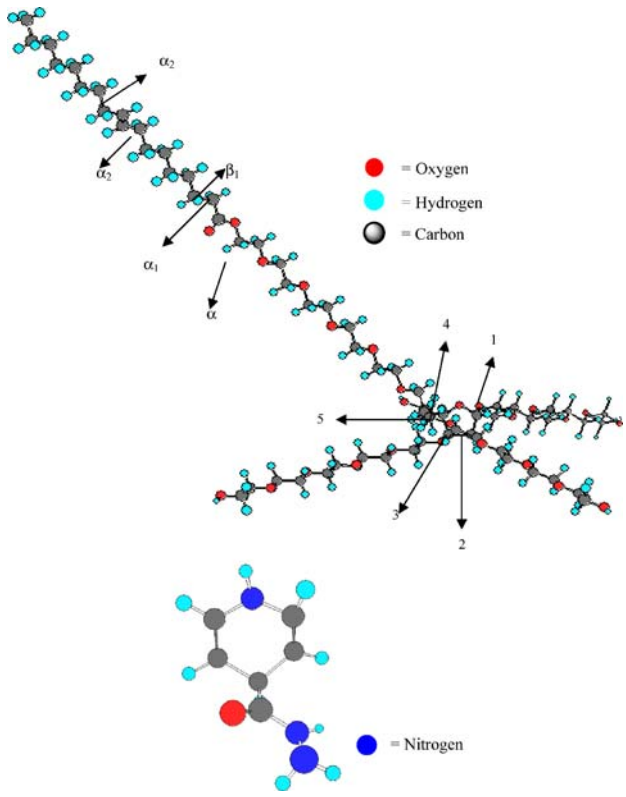

Fig. 1. Structure of Tween 80 and isoniazid.

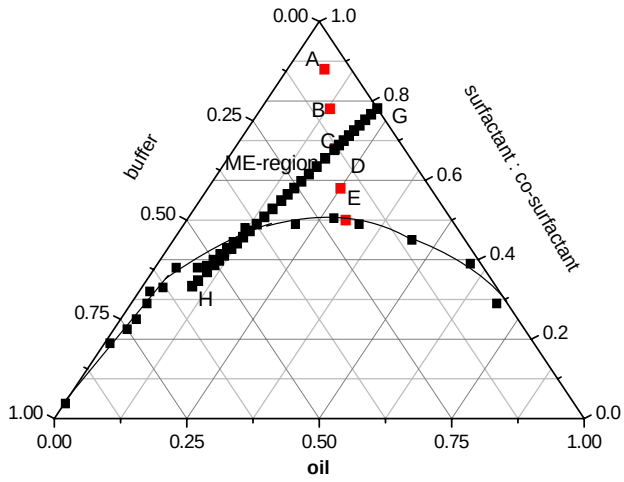

Fig. 2. Gibbs triangle (Pseudo-ternary phase diagram) showing microemulsion region of Tween 80/ethanol/oleic acid/PB pH (7.4) with Km 0.55 at 30°C. GH represents the dilution line and compositions A–E were selected for further investigations.

A number of novel implant-, microparticulate-, and various other carriers based drug delivery systems incorporating the principal antitubercular agents have been fabricated (27). In this study, an attempt has been made to construct a microemulsion system, for an antitubercular drug isoniazid (Fig. 1). A microemulsion system comprising oleic acid as an oil, a non ionic surfactant Tween 80, a short chain alkanol co-surfactant (ethanol) and phosphate buffer (PB) pH 7.4 was selected. The pseudo-ternary phase diagram has been delineated for the chosen system at a constant surfactant: cosurfactant mass ratio (Km 0.55). The gradual changes in the microstructure of microemulsion have been investigated by conductivity, viscosity, surface tension and density measurements. The influence of isoniazid on stability, optical texture and on microstructure for the formulation has also been analyzed. Selected drug loaded microemulsions have been characterized for particle size and dissolution studies at infinite dilution. FT-IR and ^{1}H NMR spectroscopy has also been used locate the possible site of drug in the microemulsion system.

MATERIALS AND METHODS

Materials

Tween 80 (polyoxyethylene sorbitan monooleate) and Isoniazid were purchased from Sigma. Absolute ethanol and Oleic acid were obtained from Merck and CDH respectively. Phosphate buffer (0.01M, pH 7.4) was used as the hydrophilic phase.

Methods

Microemulsion Preparation and Gibbs Triangle

The Gibbs triangle (pseudo-ternary phase diagram) was mapped (as shown in Fig. 2) using oil (oleic acid), surfactant (Tween 80, HLB = 15), co-surfactant (ethanol) and aqueous phase PB (pH 7.4) at 30°C ± 0.01°C with constant surfactant: co-surfactant mass ratio (Km 0.55). The temperature was

Table I. Selected Microemulsion Formulations (% (w/w))

	A	B	C	D	E
Buffer	5	9	13	17	20
Oleic acid	7	13	19	25	30
Tween 80	31	28	24	21	18
Ethanol	57	50	44	37	32

kept at 30 ± 0.01°C and was maintained by a RE320 Ecoline thermostat. Oleic acid and PB were first mixed with Tween 80, ethanol was then added to obtain the desired microemulsion compositions. The samples were prepared in a screw cap glass vials. The changes in the samples were observed visually everyday for a month. Transparent, single phase mixtures were designated as microemulsions. All the samples were stable for over 6 months, remaining clear and transparent.

Drug Incorporation in Microemulsion

Five microemulsions (ME–A to E) were selected from the single phase region of Gibbs triangle (Fig. 2) with composition as mentioned in Table I, to study their potential as drug delivery system. Isoniazid was dissolved into the preweight hydrophilic component of the system at a concentration of 0.5 and 1% (w/w) under stirring followed by addition of remaining components.

Microemulsion Characterization

Optical Transparency. The homogeneity and optical isotropy of pure and drug loaded microemulsion was examined by a cross polarizer and visual examination at room temperature. Samples were analyzed for any precipitation or phase separation in presence of drug.

Centrifugation. Stability of pure and drug loaded microemulsions were tested by carrying out centrifugation (Tarson) at 2,000 rpm for 30 min.

pH. pH of all the five selected microemulsions and the drug loaded microemulsion was determined at room temperature by Cyberscan 510 pH meter.

Oil/Buffer Partition Coefficient. Oil/buffer partition coefficient was calculated using the following equation

$$\text{Log P} = C_{oil}/C_{buffer} \quad (1)$$

where C_{oil} and C_{buffer} are the concentrations of drug in oil and drug in buffer, respectively. It was determined by dissolving 2 mg of isoniazid in 1 ml buffer. Oil was added in 1:1 ratio (v/v). The mixture was shaken for 5 min and centrifuged for 1 h. The two layers were separated and the content of isoniazid in aqueous layer (PB) was assayed by UV-visible spectrophotometer at 262 nm. The final content of drug in the lipophilic phase was calculated by subtracting the content of isoniazid in aqueous phase from initial loaded content of drug.

Table II. Different Selected Microemulsions and Their Characteristic Values

System	ω	σ (μS/cm)	pH	ϕ_c	$-\Delta G^o_{cl}(\text{KJmol}^{-1})$
ME-A	0.21	53.3	6.07	34.18	1.34
ME-B	0.45	77.6	5.56	29.31	1.69
ME-C	0.74	101.7	5.48	27.10	4.35
ME-D	1.14	142.2	5.27	26.80	6.61
ME-E	1.58	158.7	5.02		

Conductivity Measurements

The electric conductivity (σ) was measured by means of a PICO digital conductivity meter (Labindia Instruments)

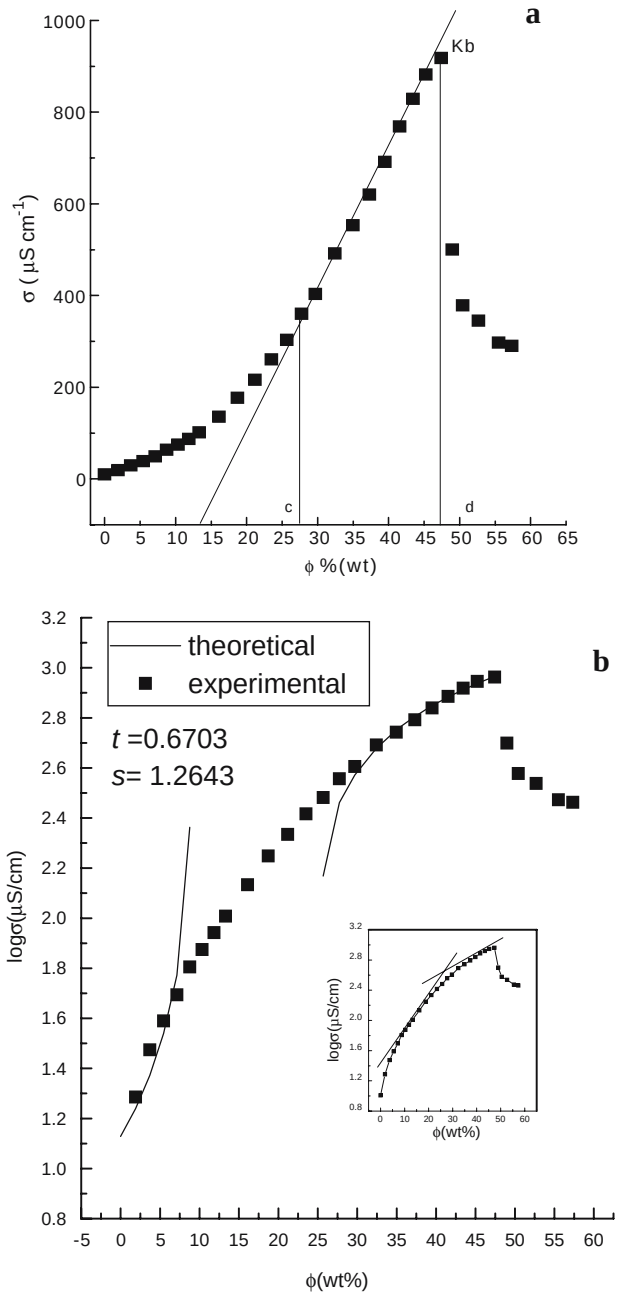

Fig. 3. Variation of **σ** (**a**) and log σ (**b**) of our component microemulsion system with Φ (% wt) along the dilution line GH (as shown in Fig. 2).

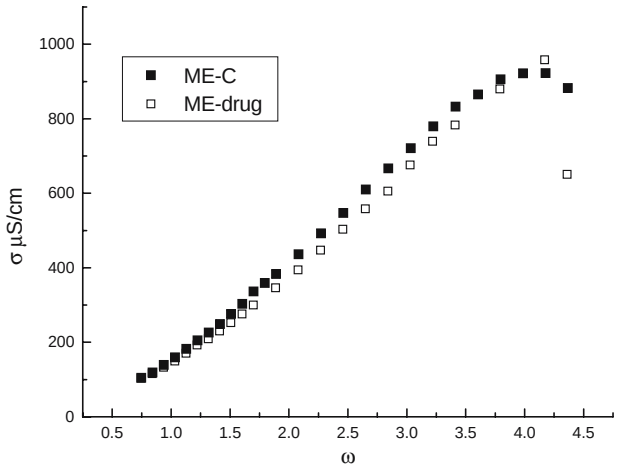

Fig. 4. Comparison of conductivity of pure ME-C and drug loaded microemulsion.

operating at 50 Hz. The error limit of conductance measurements was ±3%. The temperature was kept at 30 ± 0.01°C and was maintained by a RE320 Ecoline thermostat. Conductivity measurements were carried out by titration of oil and surfactant/cosurfactant mixture with buffer (along the dilution line GH in Fig. 2). The data was expressed in terms of wt fraction ϕ (% wt) of aqueous component which is defined as

$$\phi(\%\,\mathrm{wt}) = (\mathrm{wt\ .\ of\ buffer}/\ \mathrm{total\,wt\ .\ of\ microemulsion}) \times 100$$

Further the conductivity of selected and drug loaded microemulsions were also measured as a function of ω (=[Buffer]/[surfactant+cosurfactant]).

Viscosity Measurements

Viscosities were measured with calibrated Ubbelhode viscometer at 30 ± 0.01°C, with the experimental error of 0.5%. For each measurement, the viscometer was washed, rinsed and vacuum dried. To follow the viscous behavior of the microemulsions, flow time was measured for all the selected pure and drug loaded microemulsions (1%wt drug).

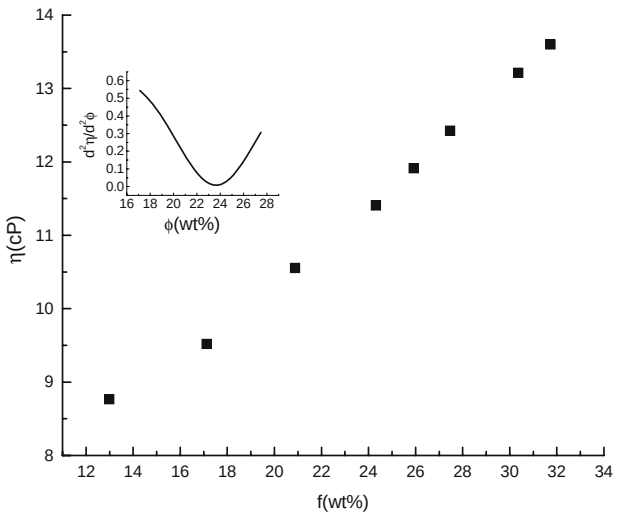

Fig. 5. Variation of dynamic viscosity as a function of weight fraction of aqueous phase. *Inset*: $d^2\eta/d^2\Phi$ as a function (Φ).

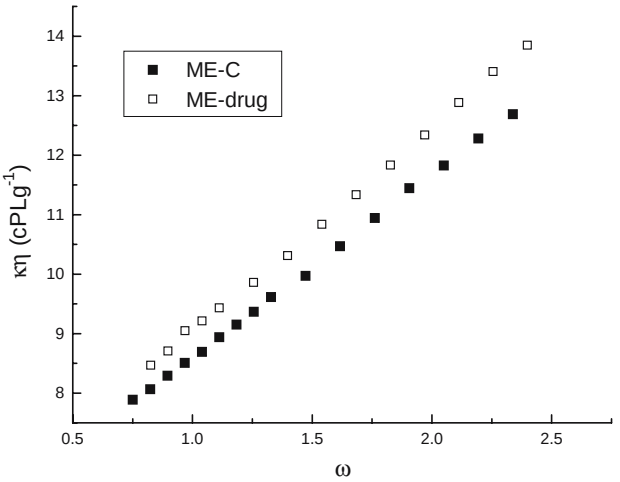

Fig. 6. Comparison of viscosity of pure ME-C and drug loaded microemulsion.

Surface Tension

Surface Tension measurements were made at 30 ± 0.01°C under atmospheric pressure by drop volume method (28). The experimental error was about ±0.05 $\mathrm{mNm^{-1}}$.

Density

Densities were measured by making use of an Austrian precisian densimeter Anton Paar (Model DMA 60) at 30 ± 0.01°C. The densimeter was calibrated before and after each set of density measurement using the density of air and pure water. Precision in the density has been estimated to be $2 \times 10^{-5}\mathrm{gl^{-1}}$.

Position Elucidation

FT-IR Analysis. FT-IR spectra of all the five selected microemulsions and of drug loaded microemulsion (0.5% and 1%wt drug) were recorded on Perkin-Elmer (RX1) FTIR spectrometer using AgCl plates, in the frequency range 4,000–350 $\mathrm{cm^{-1}}$ with 100 number scans and 4 $\mathrm{cm^{-1}}$ spectral resolution.

^{1}H NMR. ^{1}H NMR measurements were performed at 25°C on a Bruker 400 system. Chemical shifts of surfactant in

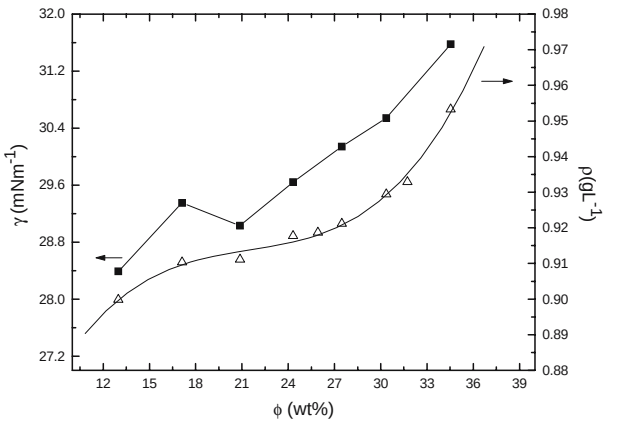

Fig. 7. Variation of Surface Tension (*filled square*) and density (*empty traingle*) with the weight fraction of hydrophilic component.

Table III. Infrared Frequencies of Different Functional Groups Present in the Components of Microemulsion

Frequency (cm^{-1})	Functional moeity
3,000–3,800	OH stretching
2,800–3,000	CH stretching
1,700	CO stretching
1,650	OH stretching
1,460	CH stretching
1,200–1,250	Ester linkages

presence of drug (0.5 and 1 wt %) were determined using D_2O as internal locking agent.

Dilutability and Particle Size Measurements. The dilutability of the microemulsions was assessed to know whether these systems would be diluted with the aqueous phase of the system without separation or not. For this purpose, selected and drug loaded microemulsions were diluted with buffer and their transparency was assessed visually. The particle size measurements (at infinite dilution) were made using laser diffraction analyzer (CILAS 1180 Liquid range (0.04–2,500 μm)).

Dissolution Studies. To perform dissolution studies, 0.55 g microemulsion containing 1% (wt) isoniazid was filled in hard gelatin capsules and introduced in 50 ml of PB (pH 7.4) maintained at 37°C ± 0.1°C. The system was stirred at constant speed at 250 rpm. The aliquot of 2 ml was withdrawn at 0, 2, 4, 8, 10, 15, 20, 30, 40, 60, 80, 100, 130 and 230 min. Each time the same amount of fresh PB (kept at the same temperature) was added to maintain the dissolution volume. The aliquots were filtered through 0.22 μm membrane filters. The drug concentrations were determined spectrophotometrically at 262 nm.

RESULTS AND DISCUSSION

In the present system, microemulsion was prepared using oleic acid (fatty acid), which induces highly permeable pathways in the stratum corneum (29,30). Tween 80 is a widely accepted nonionic surfactant, used in many pharmaceutical formulations (31–33). The co-surfactant (ethanol) is used to bring the one phase microemulsion region into experimental window of composition and temperature. The effect of alcohols on the phase behavior of nonionic microemulsion depends on the number of carbons of alcohol ($n < 3$ water soluble). The presence of alcohol overcomes the need for any additional input of energy. These properties make the components useful as vehicles for drug delivery. Alcohols can influence the formation of microemulsion by both interfacial and bulk effects (34,35).

Phase Studies

Figure 2 shows Gibbs triangle and area of existence of microemulsion for Tween 80/ethanol/oleic acid/PB. Microemulsion in the present study formed spontaneously at ambient temperature when their components were brought in contact. The phase behavior exhibits a two phase region and a large single phase region which gradually and continuously transformed from buffer rich side of binary solution (buffer/surfactant micellar phase) of Gibbs triangle towards the oil rich region. This laid an emphasis on a continuous transition from water rich compositions to oil swollen micelles. Five microemulsions (A–E) (Table I) were selected from the single-phase isotropic region and were further analyzed by conductivity, viscosity and pH. The values of measured parameters have been presented in Table II.

Conductivity Measurements

Electric conductivity was measured as a function of weight fraction of aqueous component ϕ (% wt) for the oil, surfactant/co-surfactant mixture along the dilution line GH (shown in Fig. 2). The results of variation of σ *vs* ϕ (% wt) are shown in Fig. 3a. The behavior exhibits profile characteristic of percolative conductivity (36,37). The conductivity is initially low in an oil-surfactant mixture but increases with increase in aqueous phase. The low conductivity below ϕ_c suggests that the reverse droplets are discrete (isolated droplets in a non conducting oleic medium, forming w/o microemulsion) and have little interaction. When the water content is raised above ϕ_c the value of σ increases linearly and steeply up to Kb. The interaction between the aqueous domains becomes increasingly important and forms a network of conductive channel (bicontinuous microemulsion). With further increase in water content above ϕ_d, the σ shows a sharp decrease. The system becomes turbid, that contributes to the dilution of o/w microemulsion where added buffer decrease the concentration of discrete oil droplets (19). Figure 3b depicts the variation of log σ *vs* weight fraction of water. The change in the slope of log σ (Fig. 3b) can be interpreted, as a structural transition to bicontinuous from w/o (33), nearly at $\phi = 27\%$. The transition takes place once the aqueous phase becomes continuous phase i.e. at ϕ_d. This is in line with the observation made in phase study. Thus, the σ *vs* ϕ plot illustrates occurrence of three different structures (namely w/o, bicontinuous, o/w).

From the theoretical point of view two approaches i.e. static and dynamic have been proposed for the mechanism leading to percolation (38). The first approach attributes this transition to the emergence of a bicontinuous structure i.e. an open water channel. An alternative dynamic percolation model suggests that attractive interdroplet interactions are responsible for percolative clusters and conductivity is mainly

Table IV. Different Microemulsions and Their Requencies of OH Band

ME system	OH ν (cm^{-1})	ω	Surfactant (wt%)
A	3,368.7	0.21	88
B	3,380.0	0.45	78
C	3,397.9	0.74	68
D	3,406.0	1.14	58
E	3,432.0	1.58	50

Table V. Shows Changes in the Physical Parameters of Microemulsion After Incorporation of Drug

ME System	OH υ (cm^{-1})	σ(μS/cm)	ρ(gL^{-1})	η(cP)	γ(mNm^{-1})	pH
ME C	3,397.9	101.7	0.899845	8.769	28.39	5.48
Drug(0.5%)	3,395.2	102.4	0.900323	8.987	28.44	5.23
Drug(1.0%)	3,394.4	103.6	0.901878	9.535	28.49	5.33

due to the efficient transfer of charge between spherical droplets (39). The concept of percolation is governed by scaling laws as given in Eqs. 2 and 3.

$$\sigma = A(\phi_c - \phi)^{-s} \quad \text{pre} - \text{percolation} \tag{2}$$

$$\sigma = B(\phi - \phi_c)^{t} \quad \text{post} - \text{percolation} \tag{3}$$

where A and B are free parameters and *s* and *t* are critical components. The values of critical parameters in region above and below the threshold should be $t = 1.9$ and $s = 0.6$ according to static theory. However, due to dynamic nature of the microemulsion, it has been theoretically and experimentally shown that both exponents are higher than those predicted for static case. Most of the *s* values reported lies in the range 0.7–1.6 whereas the value of *t* is more scattered (39). In the present studied system, the post percolation stage shows a good agreement between the experimental and theoretical values of log σ *vs* ϕ for water induced percolation as shown in Fig. 3b. For ME-C (along dilution line GH) value of *s and t* were found to be 1.26 and 0.67 predicting that phenomena taking place is '*static*' in nature. This attributes to the formation of continuous oil and water structures showing the presence of bicontinuous microemulsions.

Among the selected microemulsion (A–E), ME-A and ME-E were found to be unfavorable because of high surfactant content and non-dilutability respectively whereas ME-B, C, D exhibited electroconductive behavior in spite of the nonionic nature of its amphiphile (not shown here). This shows that as ω is increasing from ME-A to D, ϕ_c (percolating weight fraction) decreases (as shown in Table II), ω defines the radius of droplet. It is found that as the size of droplet is increasing the early formation of bicontinuous structure is taking place by attaining early percolating threshold. Taking into the account of energetic of clustering of droplets, in different microemulsions, ΔG^o_{cl} (standard free energy of clustering) is obtained from the relation $\Delta G^o_{cl} = RT \ln X_d$. X_d is mole fraction of droplets at percolation threshold and is defined as $X_d = n_d/n_d + n_{oil}$, where n_d and n_{oil} are the number of moles of droplet and oil. The values ΔG^o_{cl} (as shown in Table II) also confirmed that as ω is increasing the spontaneity or feasibility of clustering is being enhanced.

The variation of electric conductivity of pure (ME-C) and drug loaded microemulsion (1.0%) as a function of ω is depicted in Fig. 4. A comparison of two systems shows that drug incorporation does not affect the microstructure of the microemulsion, it only delays the gel formation and ϕ_c.

Viscosity Measurements

The dependence of dynamic viscosity, for the oil, surfactant/co-surfactant mixture along the dilution line GH (shown in Fig. 2), on the weight fraction of aqueous phase is shown in Fig. 5. The rapid change in the viscosity is probably due to the change in the microstructure of the microemulsion. The change in the internal structure could be due to either the change in the shape of droplets or may be due to the transition from w/o to bicontinuous microemulsion. It is well known that increase of volume fraction of dispersed phase in microemulsion increases viscosity of the system (40). For the system studied viscosity increases with increase in ϕ (wt% of aqueous phase). The microemulsion system thus, shows a structural change from oil continuous system to water continuous, which has higher viscosities than the former (41). The plots of η (dynamic viscosity) and $d^2\eta/d^2\phi$ reflect that the transition occurs at ~25% weight fraction of aqueous phase (Fig. 5). The transition point of conductivity and viscosity plots coincides well at ~25% weight fraction of aqueous phase and confirms the presence of percolative

Table VI. ^{1}HNMR Chemical Shifts of Tween 80 (Pure and with Different Concentrations of Drugs)

Functional Group (Fig. 1)	δ (ppm)			Δδ (ppm)	
	δ^0	$\delta^{0.5}$	$\delta^{1.0}$	$\delta^{0-0.5}$	$\delta^{0-1.0}$
C = C, ^{1}CH	5.2420	5.2430	5.2382	−0.0010	0.0030
α-CH_2 ^{4}CH	4.1287	4.1219	4.1253	0.0068	0.0034
$(CH_2CH_2O)_n$	3.6457	3.6162	3.6444	0.0029	0.0122
α_1-CH_2	2.2378	2.2403	2.2358	0.0025	0.0003
α_2-CH	1.9401	1.9411	1.9364	0.0004	0.0004
^{5}CH	1.9321	1.9330	1.9234	0.0009	0.0004
β_1-CH_2	1.5109	1.5071	1.5020	0.0038	0.0081
$(CH_2)_n$	1.2307	1.2294	1.2254	0.0013	0.0053
CH_3	0.7904	0.7897	0.7992	0.0004	0.0078

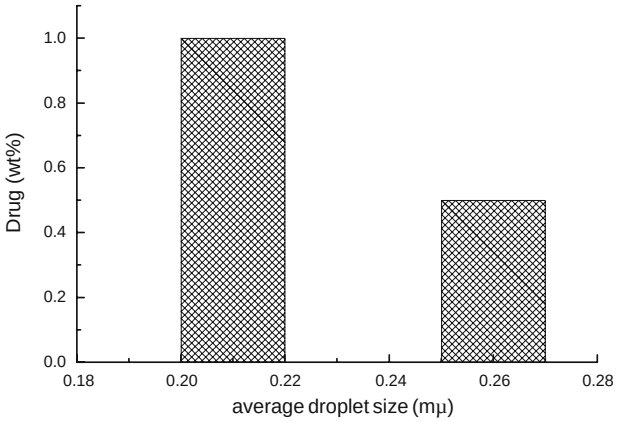

Fig. 8. Particle size of ME-C in presence of different drug content (wt%).

behavior. All the selected microemulsions showed similar trends of viscosity measurements with ω (not shown here).

In addition, the drug incorporation in ME-C made the system more viscous than the pure microemulsion as shown in Fig. 6. Difference in the viscosities is more profound for higher ω values in comparison to the dilute range. The microemulsion system is turning to be more viscous with addition of water and thus may help in the slow diffusing of drug at infinite dilution.

Surface Tension and Density

The surface tension measurements (Fig. 7) showed increment, when measured as a function of weight fraction of aqueous component, expect for the 22% weight fraction where the value suddenly decreased and thereafter a regular increase was observed. This low surface tension value showed the presence of bicontinuous microemulsion between oil and water rich system, which is because of presence of self-assembled organize microstructure in it (42). However, the density values showed a polynomial (order 2) increase with the weight fraction of aqueous component with a break at the same point owing to the structure changes in the micro-emulsion system (Fig. 7). Incorporation of drug showed a negligible change in the surface tension measurements, therefore ruling out the possibility of isoniazid molecules at the interface.

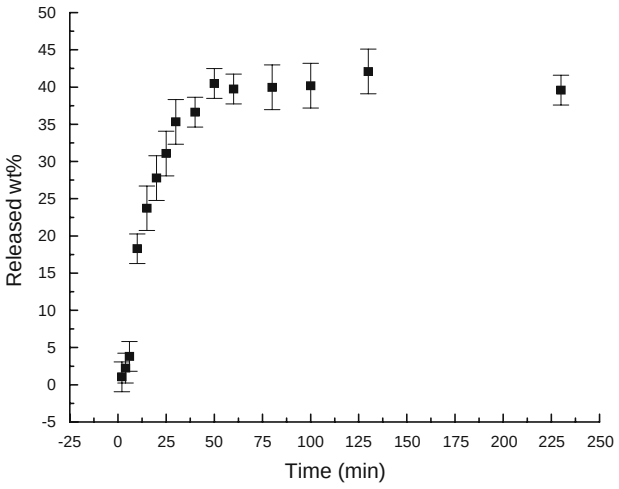

Fig. 9. Plot release rate of isoniazid from microemulsion system.

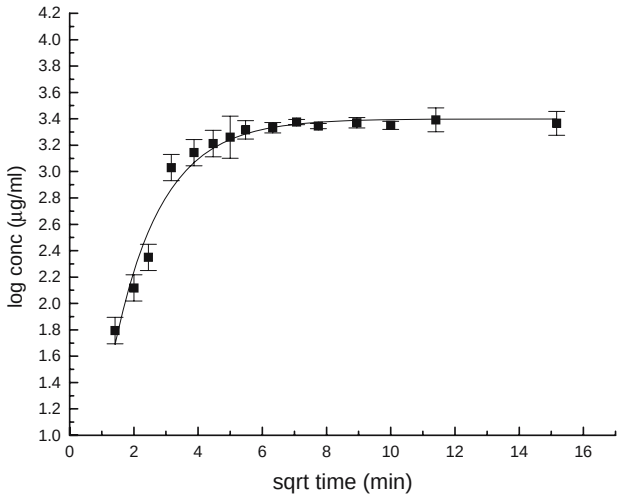

Fig. 10. Plot of log of conc. *vs.* √time, showing the typical controlled release curve.

Oil/Buffer Partition Coefficient

Using Eq. 1, the partition coefficient (Log P) of isoniazid in oil/buffer comes to -1.12 ± 0.15 (i.e. $P = 0.061$) that indicates a negligible fraction of the drug is soluble in the oil.

FT-IR Spectra

FT-IR spectra of selected microemulsions (ME-A to E) show bands of different functional groups, listed in Table III.

The first water molecules are mainly located as "interstitial" water bounded to the surfactant polar head group (43,44) and position of OH band reveals the interactions. The OH band of ME-A, B, C absorbs at lower frequency (than pure water, 3,400 cm^{-1}) and that of ME-D, E at higher frequency (Table IV). The water molecules

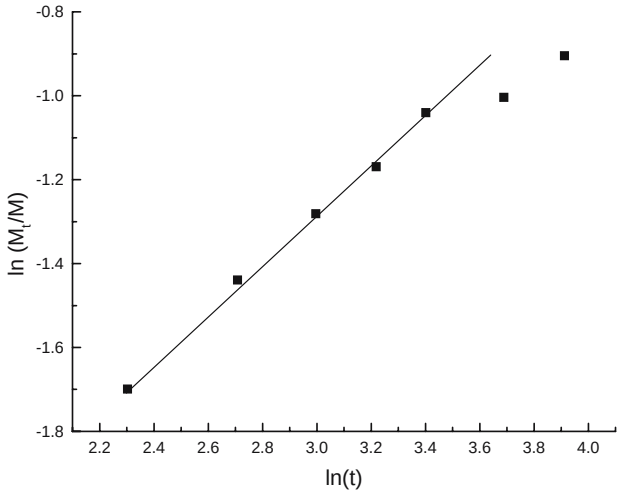

Fig. 11. Plot of relationship of $\ln(M_t/M)$ and $\ln(t)$ on the release of isoniazid from microemulsion system.

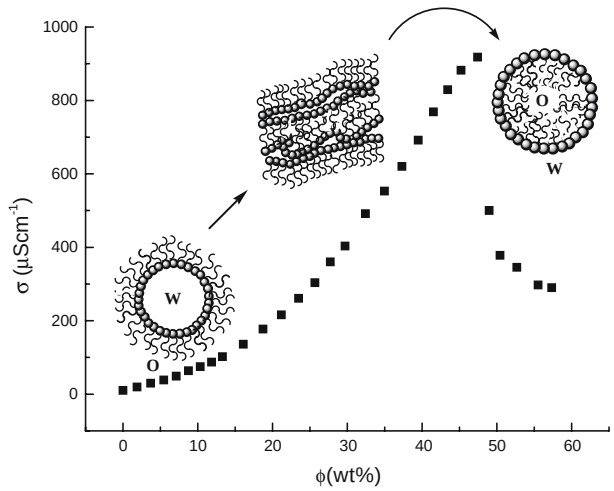

Fig. 12. Structural changes in microemulsion system with dilution.

interact strongly with surfactant molecules in A, B and C formulations, since they possess higher % (wt) of surfactant, whereas weak interactions exit in D and E formulations.

Incorporation of drug (0.5 and 1.0%) shows a negligible shift in the frequency of OH band (Table V). Even the decrease in the intensity of OH band was not substantial. This means that presence of drug is not influencing the water and surfactant head group interaction to a larger extend. This may be due to lesser availability of drug molecules near the interface and is largely present in the continuum region (due to its high solubility in aqueous media).

^{1}H NMR

In order to locate the specific site of isoniazid molecule in the microemulsion, the ^{1}H NMR spectra were recorded (33). Since the microemulsion system contains the components with long hydrocarbon and oxyethylene groups, ^{1}H NMR spectra is expected to be complex. In order to avoid the complexity, the experiments were performed with surfactant in D_2O having different amount of drugs. The main results are summarized in Table VI. Careful study of spectra of pure surfactant and in the presence of drug helps in understanding the presence of isoniazid molecules in proximity of surfactant. Since, the changes in the chemical shifts of different functional groups (Fig. 1) are very small, this limits the possibility of presence of drug near surfactant molecules, even in microemulsion system. Although at higher concentration of drug some shifts in δ value of oxyethylene groups is seen. Therefore, it may be concluded that the most of the drug is present in the dispersion medium with fairly very small amount near interface.

Dilutability and Particle Size Analysis

Both the pure (ME-C) and drug loaded microemulsions (0.5 and 1%) were tested for dilution effect. The formulations were found to remain stable on dilution up to 50% weight fraction of water and also turned turbid at infinite dilution. This indicates that there is formation of heterogeneous coarse dispersion i.e. formation of o/w emulsion from gradual transition of water in oil microemulsion (45). The particle size analysis of systems shows that the addition of 0.5% isoniazid does not have any significant influence on the size, however, 1.0% drug decreases the size to 0.21 μm (mean) from that of 0.26 μm (mean) of pure ME-C (Fig. 8). Although decrease in the particle size with addition of drug is not very significant however it is probably due to the deposition of some drug molecules at interface affecting the mobility of surfactant and thus reducing the size.

Dissolution Studies

Release Studies

Figure 9 depicts the release profile of isoniazid with time. The release increases with time up to 50 min and then becomes consistent. The M_{max} (maximum wt.% of drug) in 2 h was found to be 40%, which means the sustaining release ability of highly water soluble drug isoniazid is lowered by the microemulsion vehicle. Therefore, this microemulsion formulation helps in increases the dosage time. Although most of the drug is present in the continuum aqueous region but its the gelling (resulting higher viscosity) of microemulsion system which is guarding the diffusion of drug.

The dissolution studies of isoniazid loaded microemulsion in a hard gelatin capsules shows a typical profile of first order exponential curve (46) for logarithm of concentration *vs*. square root time (Fig. 10) and depicts the controlled release of drug (47,48).

The Kinetics of Release

The mechanism of the release of drug was analyzed by using the relationship proposed by Sinclair and Peppas as well as Ritger and Peppas (49),

$$\frac{M_t}{M} = k.t^n \qquad (4)$$

where Mt and M are the conc. of drug at time (t) and initial conc. of drug, respectively. The ratio M_t/M is the fraction of drug that has been released at time t. The parameter k is a kinetic constant and n is the exponent related to the release mechanism termed as the diffusional exponent. The value of n should be equal to 0.5 for diffusional (Fickian) release, 1 for zero-order kinetics and $0.5 < n < 1$ for anomalous (non-Fickian) release. In the present system, k and n have been calculated from the intercept and slope of the straight line in Fig. 11 The estimated value of $n = 0.5875$, indicates the release of isoniazid from microemulsion is non-Fickian (26).

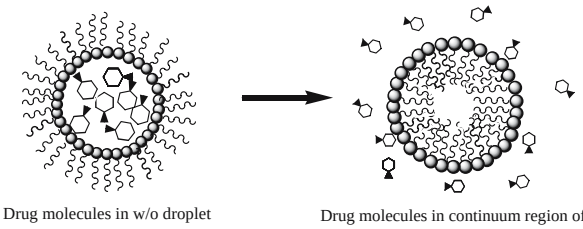

Fig. 13. Showing the probable site of drug before and after dilution.

Conclusion

The pseudo-ternary phase diagram and the area of existence of microemulsion for Tween 80/ethanol/oleic acid/ Phosphate buffer was delineated. The conductivity, viscosity, surface tension and density studies along the dilution line (in phase diagram) depict the structural transition from w/o to o/w via bicontinuous phase at ~25–27% ϕ (% weight fraction of aqueous phase) as shown in Fig. 12. Among the five selected microemulsions, ME-C was found to be optimum for the incorporation of isoniazid. After the incorporation of the drug, microemulsion remained stable and optically clear with no phase separation. The presence of drug in the microemulsion formulation is not influencing the measured physical parameters to a larger extent and therefore is not affecting the microstructure of the drug delivery vehicle. The partitioning behavior, surface tension, FT-IR, ^{1}H NMR and particle size analysis indicated that most of the drug is residing in the aqueous dispersion phase (Fig. 13). At infinite dilution the w/o microemulsion droplet changes into o/w emulsion type and there was a sustained release of isoniazid from this microemulsion drug delivery vehicle.

ACKNOWLEDGEMENTS

S.K.M. is thankful to UGC and DST India for financial assistance.

REFERENCES

1. W. A. Ristsehel. Microemulsions for improved peptide absorption from the gastrointestinal tract. Method find. *Exp. Clin.* **13**:205–220 (1991).
2. J. M. Sareiaux, L. Acar, and P. A. Sado. Using microemulsion formulations for oral delivery of therapeutic peptides. *Int. J. Pharm.* **120**:127–136 (1995).
3. P. P. Constantinides. Lipid microemulsion for improving drug dissolution and oral absorption: physical and biopharmaceutical aspects. *Pharm. Res.* **12**:1561–1572 (1995).
4. T. R. Kummaro, B. Gurley, M. A. Khan, and I. K. Reddy. Self-emulsifying drug delivery systems (SEMDDS) of co-enzyme Q_{10}: formulation development and bioavailablity assessment. *Int. J. Pharm.* **212**:233–246 (2001).
5. C. K. Kim, Y. J. Cho, and Z. J. Gao. Preparation and evaluation of biphenyl dimetyl dicarboxylate microemulsons for oral delivery. *J. Control. Release* **70**:149–155 (2001).
6. K. Kawakami, T. Yoshikawa, T. Hayashi, Y. Nishihara, and K. Masuda. Microemulsion formulation for enhanced absorption of poorly soluble drugs II. *In vivo* study. *J. Control. Release* **81**:75–82 (2002).
7. C. W. Pouton. Formulation of self-emulsifying drug delivery systems. *Adv. Drug Deliv. Rev.* **25**:47–58 (1997).
8. H. N. Bhargava, A. Narurkar, and I. M. Lieb. Using microemulsion for drug delivery. *Pharm. Technology* **1**:46–54 (1987).
9. M. Trotta, S. Morel, and M. R. Gasco. Effect of oil phase composition on the skin permeation of felodipine from o/w microemulsion. *Pharmazie* **52**:50–53 (1997).
10. M. A. Bolzinger, T. C. Carduner, and M. C. Poelman. Bicontinuous sucrose ester microemulsion: a new vehicle for tropical delivery of niflumic acid. *Int. J. Pharm.* **176**:39–45 (1998).
11. M. Kreigaard, M. J. Kemme, J. Burggraaf, R. C. Schoemaker, and A. F. Cohen. Influence of microemulsion vehicle on a cutaneous bioequivalence of a lipophilic model drug assessed by microdialysis and pharmacodynamics. *Pharm. Res.* **18**:593–599 (2001).
12. M. Kreigaard, E. J. Pederson, and J. W. Jaroszewski. NMR characterization and transdermal drug delivery potential of microemulsion system. *J. Control. Release* **69**:421–433 (2000).
13. L. Lehmann, S. Keipert, and M. Gloor. Effects of microemulsions on the stratum corneum and hydrocortisone penetration. *Eur. J.Pharm. Biopharm.* **52**:129–136 (2001).
14. K. Kriwet and C. C. Muller-Goymann. Diclofenac release from phospholipid drug systems and permeation through excised human stratum corneum. *Int. J. Pharm.* **125**:231–242 (1995).
15. M. Trotta. Infleunce of phase transformation on indomethacin release from microemulsions. *J. Control. Release* **60**:399–405 (1999).
16. M. E. Dalmora, and A. G. Oliveria. Inclusion complex of peroxicam with β-cyclodextrin and incorporation in heaxdecyltrimethyl ammonium bromide based microemulsions. *Int. J. Pharm.* **184**:157–164 (1999).
17. F. Pattarino, E. Marengo, and M. R. Gasco. Experimental design and partial least square in the study of complex mixtures: microemulsions as drug carriers. *Int. J. Pharm.* **91**:157–165 (1993).
18. P. Kumar and K. L. Mital. *Handbook of microemulsion: science and technology*, Marcel Dekker, New York, 1999.
19. F. Podlogar, M. Gašperlin, M. Tomšič, A. Jamnik, and M. Bešter-Rogač. Structural characterization of water-Tween 40®–Imwitor 308®–isopropyl myristate using different experimental methods. *Int. J. Pharm.* **276**:115–128 (2004).
20. A. Lopez, F. Linares, C. Cortell, and M. Herraez. Comparative enhancer effects of Span 20® with Tween 20® and Azone® on the *in vitro* percutaneous penetration of compounds with different lipophilicities. *Int. J. Pharm.* **202**:133–140 (2000).
21. J.-Y. Fang, S.-Y. Yu, P.-C. Wu, Y.-B. Huang, and Y.-H. Tsai. In vitro skin permeation of estradiol from various proniosome formulations. *Int. J. Pharm.* **215**:91–99 (2001).
22. A. H. Kibbe. *Handbook of Pharmaceutical Excipients*, 3rd ed. Pharmaceutical, London, 2000.
23. M. J. Lawerence and G. D. Rees. Microemulsion based media as novel drug delivery systems. *Adv. Drug Deliv. Rev.* **45**:89–121 (2000).
24. J. Kreuter. Nanoparticles. In *Colloidal Drug Delivery Systems*, Marcel Dekker, New York (1994).
25. A. T. Florence and D. Attwood. *Physicochemical Principles of Pharmacy*, 3rd ed. Macmillan, London.
26. R. Guo, S. Qian, J. Zhu, and J. Qian. The release of cephanone in CTAB/n-$C_5H_{11}OH/H_2O$ system. *Colloid. Polym. Sci.* **284**:468–474 (2006).
27. L. C. Toitdu, V. Pillay, and M. P. Danckwerts. Tuberculosis chemotherapy: current drug delivery approaches. *Resp. Res.* **7**:118–136 (2006).
28. J. L. Lando and H. T. Oakley. Tabulated correction factors for the drop-weight-volume determination of surface and interracial tensions. *J. Colloid Interface Sci.* **25**:526–528 (1967).
29. L. K. Pershing, G. E. Parry, and L. D Lambert. Disparity of in vitro and *in vivo* oleic acid-enhanced β-estradiol percutaneous absorption across human skin. *Pharm. Res.* **10**:1745–1750 (1993).
30. H. Tanojo, H. E. Junginger, and H. E. Boddé. *In vivo* human skin permeability enhancement by oleic acid: transepidermal water loss and Fourier-transform infrared spectroscopy studies. *J. Control. Release* **47**:31–39 (1997).
31. S. Peltola, P. J. Saarinen-Savolainen, T. M. Suhonen, and A. Urtti. Microemulsions for topical delivery of estradiol. *Int. J. Pharm.* **254**:99–107 (2003).
32. N. Subramanium, S. Ray, S. K. Ghosal, R. Bhadra, and S. P. Moulik. Formulation design of self-microemulsifying drug delivery systems for improved oral bioavailability of celecoxib. *Biol. Pharm. Bull.* **27**:1993–1999 (2004).
33. F. F. Lv, L. Q. Zheng, and C.-H. Tung. Phase behavior of the microemulsions and the stability of the chloramphenicol in the microemulsion-based ocular drug delivery system. *Int. J. Pharm.* **301**:237–246 (2005).
34. K. V. Schubert and E. W. Kaler. Nonionic microemulsions. *Phys. Chem.* **100**:190–205 (1996).
35. R. G. Alany, T. Rades, S. Agatonovic-Kustrin, N. M. Davies, and I. G. Tucker. Effects of alcohols and diols on the phase behavior of quaternary systems. *Int. J. Pharm.* **196**:141–145 (2000).

36. S. K. Mehta and K. Bala. Tween based microemulsions: a percolation view. *Fluid Phase Equilibra* **172**:197–209 (2000).
37. G. S. Grest, I. Webman, and S. A. Safran. Dynamic percolation in microemulsions. *Phys. Rev. A* **33**(4):2842–2845 (1986).
38. B. Lagourette, J. Peyrelasse, C. Boned, and M. Clausse. Percolative conduction in microemulsion type systems. *Nature* **281**:60–62 (1979).
39. S. K. Mehta and K. Bala. Volumetric and transport properties in microemulsions and the point of view of percolation theory. *Phys. Rev. E.* **51**:5732–5737 (1995).
40. K. E. Bennett, J. C. Hatfield, H. T. Davis, C. W. Macosko, and L. E. Seriven. Viscosity and conductivity of microemulsions. In: Robb, I. D. (ed.), *Microemulsions*, Plenum, New York, pp 65–84 (1982).
41. R. K. Mitra and B. K. Paul. Physicochemical investigations of microemulsification of eucalyptus oil and water using mixed surfactants (AOT + Brij35) and butanol. *J. Colloid Inter. Sci.* **283**:565–577 (2005).
42. M. E. Leser, W. C. Evert, and W. G. M. Agterof. Phase behaviour of lecithin–water–alcohol–triacylglycerol mixtures. *Colloids Surf A.* **116**:293–308 (1996).
43. F. Aliotta, P. Migliardo, D. I. Donato, V. Turco Liveri, E. Bardez, and B. Larry. Local hydration effects in reversed micellar aggregation. *Progr. Colloid Polym. Sci.* **89**:258–262 (1992).
44. V. Arcoleo, M. Goffredi, and V. Turco Liveri. Physicochemical characterization of copper (II) bis(2-ethylhexyl) sulfosuccinate reversed micelles. *J. Colloid Int. Sci.* **198**:216–223 (1998).
45. H. M. El-Laithy. Preparation and physicochemical characterization of dioctyl sodium dulfosuccinate (Aersol OT) microemulsion for oral drug delivery. *AAPS PharmSciTech* **4**(Article 11): 1–10 (2003).
46. H. Dai, Q. Chen, H. Qin, Y. Guan, D. Shen, Y. Hua, Y. Tang, and J. Xu. A temperature-responsive copolymer hydrogel in controlled drug delivery. *Macromolecules* **39**:6584–6589 (2006).
47. N. Wakiyama, K. Juni, and M. Nakano. Preparation and evaluation *in vitro* of polylactic acid microspheres containing local anesthetics. *Chem. Pharm. Bull.* **29**:3363–3368 (1981).
48. L. Zhang, X. Sun, and Z.-R. Zhang. An investigation on liver-targeting microemulsions of norcantharidin. *Drug Deliv.* **12**:289–295 (2005).
49. C. Washington. Drug release from microdisperse systems: a critical review. *Int. J. Pharm.* **58**:1–12 (1990).